Journal of Ginseng Research 46 (2022) 780–789

Contents lists available at ScienceDirect

Journal of Ginseng Research

journal homepage: https://www.sciencedirect.com/journal/journal-of-ginseng-research

Research Article

Compound K attenuates hyperglycemia by enhancing glucagon-like peptide-1 secretion through activating TGR5 via the remodeling of gut microbiota and bile acid metabolism

Fengyuan Tian [a, 1], Shuo Huang [a, 1], Wangda Xu [a], Lan Chen [a], Jianming Su [b], Haixiang Ni [c], Xiaohong Feng [c], Jie Chen [c], Xi Wang [d, *], Qi Huang [c, **]

[a] First School of Clinical Medicine, Zhejiang Chinese Medical University, Hangzhou, Zhejiang, China
[b] Department of Emergency, First Affiliated Hospital of Zhejiang Chinese Medical University, Hangzhou, Zhejiang, China
[c] Department of Endocrinology, First Affiliated Hospital of Zhejiang Chinese Medicine University, Hangzhou, China
[d] Central Laboratory, First Affiliated Hospital of Zhejiang Chinese Medical University, Hangzhou, China

ARTICLE INFO

Article history:
Received 13 December 2021
Received in revised form
25 February 2022
Accepted 29 March 2022
Available online 31 March 2022

Keywords:
Compound K
GLP-1
Bile acids
TGR5
Enteroendocrine cells

ABSTRACT

Background: Incretin impairment, characterized by insufficient secretion of L-cell-derived glucagon-like peptide-1 (GLP-1), is a defining step of type 2 diabetes mellitus (T2DM). Ginsenoside compound K (CK) can stimulate GLP-1 secretion; however, the potential mechanism underlying this effect has not been established.

Methods: CK (40 mg/kg) was administered orally to male db/db mice for 4 weeks. The body weight, oral glucose tolerance, GLP-1 secretion, gut microbiota sequencing, bile acid (BA) profiles, and BA synthesis markers of each subject were then analyzed. Moreover, TGR5 expression was evaluated by immunoblotting and immunofluorescence, and L-cell lineage markers involved in L-cell abundance were analyzed.

Results: CK ameliorated obesity and impaired glucose tolerance in db/db mice by altering the gut microbiota, especially *Ruminococcaceae* family, and this changed microbe was positively correlated with secondary BA synthesis. Additionally, CK treatment resulted in the up-regulation of CYP7B1 and CYP27A1 and the down-regulation of CYP8B1, thereby shifting BA biosynthesis from the classical pathway to the alternative pathway. CK altered the BA pool by mainly increasing LCA and DCA. Furthermore, CK induced L-cell number expansion leading to enhanced GLP-1 release through TGR5 activation. These increases were supported by the upregulation of genes governing GLP-1 secretion and L-cell differentiation.

Conclusions: The results indicate that CK improves glucose homeostasis by increasing L-cell numbers, which enhances GLP-1 release through a mechanism partially mediated by the gut microbiota-BA-TGR5 pathway. Therefore, that therapeutic attempts with CK might be useful for patients with T2DM.

1. Introduction

Incretin impairment is a common disturbance in type 2 diabetes mellitus (T2DM), which presents mostly as inadequate glucagon-like peptide-1 (GLP-1) secretion by L-cells [1]. GLP-1 is a powerful gut hormone involved in glucose metabolism and is recognized for its critical role in insulin secretion during food intake, in gastrointestinal motility, and in gastropancreatic secretions. GLP-1-based treatments and have been widely used in clinical settings. Recently, expanding L-cell numbers has been reported to be a promising alternative to augmenting GLP-1 bioavailability, thereby overcoming incretin impairment from the cell fate source [2,3]. A complex and precise mechanism is involved in enforcing the continuous intestinal epithelial layer renewal to expand the L-cell population [4].

L-cell differentiation in crypts is a continuous process originating from early secretory progenitors that express a specific

* Corresponding author. Central Laboratory, First Affiliated Hospital of Zhejiang Chinese Medicine University, Hangzhou, 310006, China.
** Corresponding author. Department of Endocrinology, First Affiliated Hospital of Zhejiang, Chinese Medicine University. Hangzhou, 310006, China.
E-mail addresses: wangxi@zcmu.edu.cn (X. Wang), hzhq1987@163.com (Q. Huang).
[1] These authors contributed equally to this manuscript.

https://doi.org/10.1016/j.jgr.2022.03.006

lineage marker, Math1 [5]. To fulfill enteroendrocrine functions, cell progenitors enter the specialized enteroendocrine fate with the onset of Ngn3 expression [6]. In the next phase, some of these secretory cell progenitors upregulate NeuroD1 expression [7], which is unique to enteroendocrine cells (EECs), and this process relies on the common molecular markers Foxa1 and Foxa2 to direct maturation toward L-cells [8]. Mature L-cells account for merely 0.5% of intestinal epithelial cells, and preproglucagon (Gcg) is considered a marker for L-cell maturation [9]. Recent advances indicate that intestinal epithelial cells with overall differentiation potential can evolve into various lineages, including EECs and L-cells [10]. Hence, elucidating the mechanism by which intestinal epithelial cells are converted to L-cells is essential.

Gut microbiota, a huge symbiotic community inside the intestinal tract, has been identified as a causal factor for obesity and diabetes, both sharing a vital feature—an increase in the *Firmicutes*/*Bacteroides* ratio [11]. Among gut microbiota-produced metabolites, bile acids (BAs) are the dominant ones. BAs are produced during cholesterol catabolism in the liver form the BA pool. They regulate glycolipid metabolism and immune responses, deeply involved in incretin effect [12]. BAs synthesis is mediated via both, the classical and alternative pathways, principally by initiating BA conjugation. In the intestine, conjugated BAs undergo a series of deconjugation, dehydrogenation, and dihydroxylation. Gut microbiota-dependent biotransformations include the conversion of cholic acid (CA) and chenodeoxycholic acid (CDCA) to deoxycholic acid (DCA) and lithocholic acid (LCA), respectively. It is worth noting that secondary BAs showing the highest affinity to the bile acid receptor-Takeda G protein-coupled receptor 5 (TGR5) are LCA and DCA [13]. TGR5 expression has been identified along the entire gastrointestinal tract, where its activation regulates multiple intestinal homeostatic functions, including gut hormone release, gastrointestinal peristalsis, and local immune responses [14]. Furthermore, the increase in secondary BAs triggers the activation of TGR5 and promotes the regeneration of L-cells in intestinal organoids, which impels more intestinal epithelial cells to convert into GLP-1-producing cells, supported by the upregulation of transcription factors dominating L-cell maturation [15].

Panax ginseng Meyer, a famous traditional herb, has been used in East Asia for millennia to treat diabetes. Ginsenosides are major bioactive constituents of ginseng and have diverse pharmacological benefits, such as improving and reversing hyperglycemia and obesity. Compound K (CK), a major metabolite of ginsenoside Rb1, Rb2, Rc, and Rd, is synthesized by gut microbiota metabolism after oral administration of ginseng [16]. Following absorption in the intestine, CK helps to achieve glycemic control though improving glucolipid metabolism and insulin sensitivity [17]. Furthermore, CK was considered a native TGR5 agonist in a previous study [18]. We previously confirmed that CK facilitates GLP-1 secretion under glucotoxicity in vitro by alleviating the impaired differentiation of L-cells [19]; however, this specific mechanism remains to be further explored and validated in vivo, taking the microbiota-BA-TGR5 axis into consideration. Herein, the role of CK in the expansion of the L-cell population and the enhancement of GLP-1 release by remodeling of the microbiota-BA-TGR5 axis in db/db mice were assessed.

2. Materials and methods

2.1. Animals and treatments

4-week wild-type C57BL/6 J male mice (15–20 g, n = 6) and obese-diabetic Leprdb/db (db/db, B6.BKS(D)-leprdb/J) male mice (35–40 g, n = 12) were obtained from Shanghai SLAC Laboratory Animal Co., Ltd (Shanghai, China). The mice were housed at a temperature of 25 ± 2 °C, a humidity of 60 ± 5%, a12:12 h light/dark diurnal cycle, with food and water ad libitum. CK (molecular weight 622.87 Da, purity ≥99.0%) was procured from Shanghai Winherb Medical Science Co., Ltd. (Shanghai, China). After a week of acclimatization, the mice were randomly assigned to three groups, namely, the control group, the db/db group, and the CK group. The CK group was administrated with 40 mg/kg of CK orally once a day, while the control and the db/db groups were gavaged with an equal volume of vehicle solution [0.5% sodium carboxymethyl cellulose (CMC-Na)]. Regarding supplemental gavage feeds, the mice were weighed every 2 days, and the gavage doses were adjusted according to the body weight. The dosage of CK was based on mouse CK dosages reported in previous studies [20]. After 4 weeks of treatment, the mice were euthanized. Animal welfare and experimental procedures were authorized by the Board of Animal Study of Zhejiang Chinese Medical University (approval no.20210104–07).

2.2. Oral glucose tolerance test (OGTT)

After overnight fasting, each mouse was given an oral gavage of 2 g/kg of 50% dextrose. Plasma glucose was measured from the tail vein blood samples before and 15, 30, 60, and 90 min after the oral dextrose load using a One-Touch FastTake glucometer (Accu-Check, Roche, IN, USA). Area under the blood glucose curve (AUC) was derived using the trapezoidal rule.

2.3. Insulin and GLP-1 analysis

Blood samples were collected by extirpating the eyeballs following sacrifice after 4 weeks of administration. Serum was then acquired by centrifuging the blood samples at 4 °C (1200 g, 20 min). Insulin ELISA kit and GLP-1 ELISA kit were purchased from Millipore (MA, USA). The concentrations of insulin and GLP-1 in the serum samples were quantified by ELISA according to the kits' instruction.

2.4. 16 S rRNA sequencing of the whole gut microbiota

Fresh feces were collected, immediately frozen, stored at −80 °C, and subjected to 16 S rRNA sequencing. Microbial genomic DNA extraction was performed with a DNeasyPowerSoil kit (Qiagen, CA, USA). PCR amplicons were purified with a PCR purification kit (Thermo Fisher Scientific, MA, USA) and then quantified, pooled and sequenced with the TruSeqTM DNA PCR-Free Sample Prep kit (Illumina, CA, USA) with PE150 strategy using the standard protocol. The resulting bacterial sequence fragments were sequenced by the Illumina HiSeq X-ten platform using the PE300 mode within a NovaSeq sequencing system. High-quality reads were assigned to respective samples, aligned, and clustered into operational taxonomical units (OTUs) with >97% sequence similarity that simultaneously performs chimaera filtering and OTU clustering. The bacterial sequences were assigned taxonomically based on the SILVA and NCBI databases. Alpha and beta diversity metrics of the samples were calculated using the R package Vegan. Alpha-diversity metrics, including Chao1 and Shannon indices, were used to assess microbial community structures and were computed using R software. Non-metric multidimensional scaling analysis (NMDS) and the principal coordinate analysis (PCoA), based on the unweighted UniFrac distance matrices, were visualized by R software to analyze communities and phylogenesis for the beta diversity.

2.5. BA metabolite profile assessment

The BA pool size and composition of each serum sample were determined using ultra-high performance liquid chromatograph-mass spectrometry (UPLC-MS) as previously reported [21]. Briefly, an aliquot of 50 μL of serum sample was mixed with 150 μL of 75% methanol and centrifuged (4 °C, 12000g) for 10 min to precipitate proteins. The supernatant was transferred to an autosampler vial for nitrogen drying. Then, the residue was redissolved in a 100 μL mixture containing 0.01% acetic acid and 5 mM ammonium methanol/acetate (55:45, v/v), followed by centrifugation at 4 °C (20000 g, 10 min). After filtration, the liquid samples were directly injected and analyzed with an Acquity UPLC I-Class system (Waters, MA, USA). Standard solutions were mixed at appropriate concentrations for calibration and tested once every ten samples for quality control.

2.6. Immunoblotting analysis

Ileal tissues were homogenized in radioimmune precipitation (RIPA) lysis buffer (Beyotime, Shanghai, China) containing 1 mM phenylmethylsulfonyl fluoride (PMSF) (Beyotime) on ice. The total protein concentration was quantified with a BCA Protein Assay Kit (Thermo Scientific). Denatured proteins of lysates separated by 10% SDS-PAGE were electrotransferred to polyvinylidene difluoride (PVDF) membranes (Millipore). Next, the membranes were blocked with 5% bovine serum albumin (BSA) and then incubated with the individual primary antibodies TGR5 (1:1000, Abcam, MA, USA) overnight at 4 °C. After washing three times with Tris-buffered saline containing Tween 20 (TBST), the membranes were incubated with horseradish-peroxidase-conjugated secondary antibodies (1:2000, Cell Signalling Technology, MA, USA) at room temperature for 2 h. Subsequently, the antigen-antibody complexes were visualized by enhanced chemiluminescence (ECL) with detection reagents (Bio-Rad, CA, USA). ImageJ was used to process blot images and quantify band intensities.

2.7. Immunofluorescence staining

Frozen ileal sections (5 μm) were fixed for 10 min in 4% formaldehyde and then blocked with 4% BSA for 1 h, followed by overnight staining with the primary antibodies against Gcg (1:100, Cell Signalling Technology) and TGR5 (1:100, Abcam). Following primary antibody incubation, the samples were incubated overnight with Alexa Fluor 488—labeled goat anti-rabbit IgG secondary antibody (1:250, Invitrogen, CA, USA). Subsequently, nuclear staining was performed using DAPI (Sigma-Aldrich, MO, USA). Stained specimens were observed using an LSM700 confocal microscope (Carl Zeiss, Oberkochen, Germany), and ImageJ was utilized to measure fluorescence intensity and cell count.

2.8. Quantitative RT-PCR analysis

Following the manufacturer's protocol, total RNA was extracted from ileal and liver tissues using a mini RNA extraction kit (Qiagen) and then reverse-transcribed into cDNA using the SuperScript III kit (Thermo Fisher Scientific). Real-time qPCR was performed on a real-time PCR System (Bio-Rad) using SYBR green assays and the experiment was performed in triplicate. We selected Glyceraldehyde-3-phosphate dehydrogenase (GAPDH) as the endogenous control gene. Mouse primer sequences were described presented in Supplementary Table 1.

2.9. Statistics

Data were expressed as the mean and standard error of the mean (s.e.m.). Differences in the mean values among the three groups were evaluated using one-way analysis of variance (ANOVA) and Turkey's multiple comparisons post hoc analysis using GraphPad Prism version 8.0 software (GraphPad, CA, USA). *P*-values < 0.05 were considered statistically significant (* < 0.05; ** < 0.01).

3. Results

3.1. CK treatment ameliorates obesity-diabetes

To investigate the underlying mechanisms of CK on enteroendocrine repair, db/db mice were orally gavaged with CK for 4 weeks. CK administration resulted in considerable improvement of multiple features of T2DM. The bodyweight, liver weight, and liver/body weight ratio of db/db mice were significantly increased compared to the wild-type control mice (Fig. 1A–C). In contrast, treated mice attenuated leptin receptor-mutated increase of body weight from day 6 of the start of treatment (Fig. 1A and B), a loss that could be ascribed to decreased fat mass. Analysis of glucose homeostasis parameters showed that spontaneous hyperglycemia (Fig. 1D and E) and insulin resistance (Fig. 1F and G) were observed in db/db mice. On the other hand, the CK-treated mice exhibited a reduction in blood glucose level with reduced AUC in OGTT (Fig. 1D and E) and improved insulin sensitivity (Fig. 1F and G). Furthermore, insufficient GLP-1 in db/db mice was as expected, while the 4-week CK treatment notably improved GLP-1 profiles (Fig. 1H), indicating that CK acted as an incretin secretagogue to relieve hyperglycemia.

3.2. CK-modulated gut microbial composition in db/db mice

Since the development of T2DM has been linked to gut microbiota disturbance, 16 S genome sequencing was performed to explore the overall structural changes of gut microbiota in response to CK using fecal samples of control, untreated db/db, and CK-treated mice. The metagenomic analysis determined that CK-treated mice presented lower Chao1 and Shannon indices compared to db/db mice, reflecting more homogeneous populations of bacteria in the CK group (Fig. 2A and B). Besides, PCoA and NMDS revealed distinct differences in the gut microbiome between the three groups, which implied the dissimilarity of gut microbiome after CK intervention (Fig. 2C and D).

The taxonomic distribution of the gut microbiota at the phylum and family levels was determined (Fig. 2E and F). Analysis at the phylum level revealed a moderate increase in *Firmicutes* proportion at the expense of *Bacteroidetes* proportion in db/db mice compared to the control, as well as an increase in the *Firmicutes/Bacteroidetes* ratio (Fig. 2G). In contrast, CK treatment substantially decreased the *Firmicutes/Bacteroides* ratio (Fig. 2G). Further analysis at the family level revealed reductions in the abundances of *Lactobacillaceae*, *Akkermansiaceae*, and *Ruminococcaceae* in db/db mice compared to control mice and significant increases in the abundances of members from *Bacteroidaceae* and *Enterococcaceae* (Fig. 2H). In addition, the abundance of *Lactobacillaceae*, *Akkermansiaceae*, *Lachnospirace*, and *Ruminococcaceae* were notably enhanced, while that *Bacteroidaceae* and *Enterococcaceae* was decreased by CK compared to db/db mice (Fig. 2H). Collectively, these findings imply that CK treatment resulted in the remodeling of the gut microbiota in db/db mice, with a restoration of the relative abundance of *Ruminococcaceae* family, which may evoke the accumulation of secondary BAs.

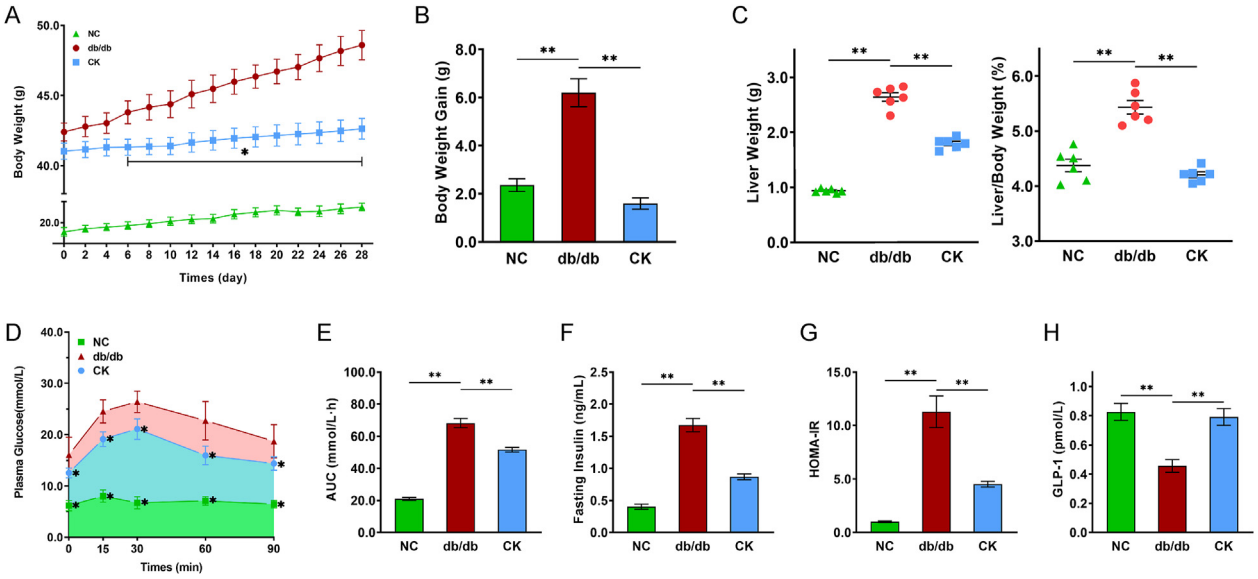

Fig. 1. CK improves glucose homeostasis partially through enhancing the GLP-1 secretion in db/db mice. 4-Week-old male db/db mice were treated with CK, with wild-type C57BL/6 J mice used as controls. Body weight (A), Body weight gain (B), liver weight and liver/body ratio (C) were observed. Results of the oral glucose tolerance test (OGTT) performed at the end of the study (D), and the calculated average changes from baseline in the area under the curve (AUC) (E). Insulin levels (F) after overnight fasting following CK treatment, and homeostasis model assessment of insulin resistance was calculated as HOMA-IR (G). Serum GLP-1 levels (H). Data are presented as the mean ± s.e.m., n = 6 per group. $^{*}P < 0.05$, $^{**}P < 0.01$ versus the db/db group.

3.3. CK treatment regulates bile acid synthesis and remodels the circulating bile acid profiles

Gut microbiota has been identified as a vital predictor of BA profiles, and alterations in the enterohepatic circulation have a causal role in glycometabolism by triggering GLP-1 secretion [12]. Conjugated primary BAs are taken up in the distal ileum. Unabsorbed primary BAs serve as substrates for microbial metabolism and undergo bioconversion into secondary BAs, which then enter to the circulation. As depicted in Fig. 3A, along this process, CYP7A1 and CYP7B1 are involved in bile acid synthesis as the initiators of the classical and alternative pathways, respectively. Indeed, multiple enzymes have been implicated in the formation of bile acids, including CYP27A1 and CYP8B1 [22]. Previous studies have reported that modulating BA synthesis to regulate BA signaling markedly influences glycolipid metabolism [23]. Thus, the expression levels of multiple key enzymes involved in hepatic BA synthesis were investigated. In db/db group, CYP7A1 and CYP27A1 were significantly elevated, whereas CYP7B1 and CYP27A1 were induced (Fig. 3B). CK contributed to the upregulation of CYP7B1 and CYP27A1 and a non-significant decrease in CYP8B1 expression (Fig. 3B), which confirmed the regression of the alternative pathway.

Ruminococcaceae family serves as a specific link to carry out the 7α-dehydroxylation step that dominates the generation of LCA and DCA [24]. To further characterize the effect of CK on BA profiles under the influence of gut microbiota, UPLC-MS-based targeted metabolomics approach was applied to analyze the BAs in the serum. The heterogeneity of serum BA profiles can be visualized in the OPLS-DA score plot, which displayed the differences between the three groups (Fig. 3C). Metabolomics analysis revealed that the accumulation of total BAs declined in db/db mice compared to control mice, while no differences emerged between CK-treated and untreated groups. Both the ratios of free-status to conjugated, or secondary to primary BA were increased with CK intervention compared with the db/db group (Fig. 3D and E). In the db/db group, CA, CDCA, ACA, LCA, DCA, UDCA, HDCA, TαMCA, and TβMCA levels were lower, whereas the TCA level was increased. Serum TαMCA, TβMCA, CA, and ACA were significantly higher in the CK-fed mice than in db/db mice (Fig. 3F). Furthermore, CK treatment resulted in the restoration of DCA and LCA levels (Fig. 3F). Therefore, CK intervention resulted in the conversion of primary BAs to secondary BAs, thereby massively increasing DCA and LCA levels.

3.4. TGR5 activation is responsible for the beneficial effects of CK

The preceding data established that the accumulation of LCA and DCA enhanced GLP-1 release, and both were involved in TGR5 activation. In the luminal environment, TGR5 signaling represses inflammation, leading to the preservation of the intestinal barrier [25,26]. Therefore, we hypothesized that the administration of CK could potentially exert the reported anti-diabetic effect on enteroendocrine cells through the microbiota-BA axis and downregulate TGR5 expression. The expression of TGR5 in the ileum of db/db mice was lower compared to the control mice, whereas CK-treated mice had a marked improvement in TGR5 expression (Fig. 4A). Immunofluorescence images also displayed that the number of TGR5-positive ileal cells located in the submucosal ganglia increased dramatically following CK treatment (Fig. 4B). Our data, therefore, indicate that enhanced secretion of GLP-1 is dependent on the direct activation of basolateral TGR5 receptors. These data also demonstrate that the disruption of TGR5 expression is linked to incretin impairment in mice with L-cell injury and that CK normalizes reduced TGR5 expression in response to hyperglycemia and inflammation, which is required for BA-mediated L-cell restoration.

3.5. CK amplifies the abundance and differentiation of L-cells

Secretory and absorptive cells of the intestinal epithelial layer have different functions. Hes1 and Math1 are the labeled markers of absorptive and secretory lineages, respectively. To test whether CK alters the proportion of secretory and absorptive cells, the

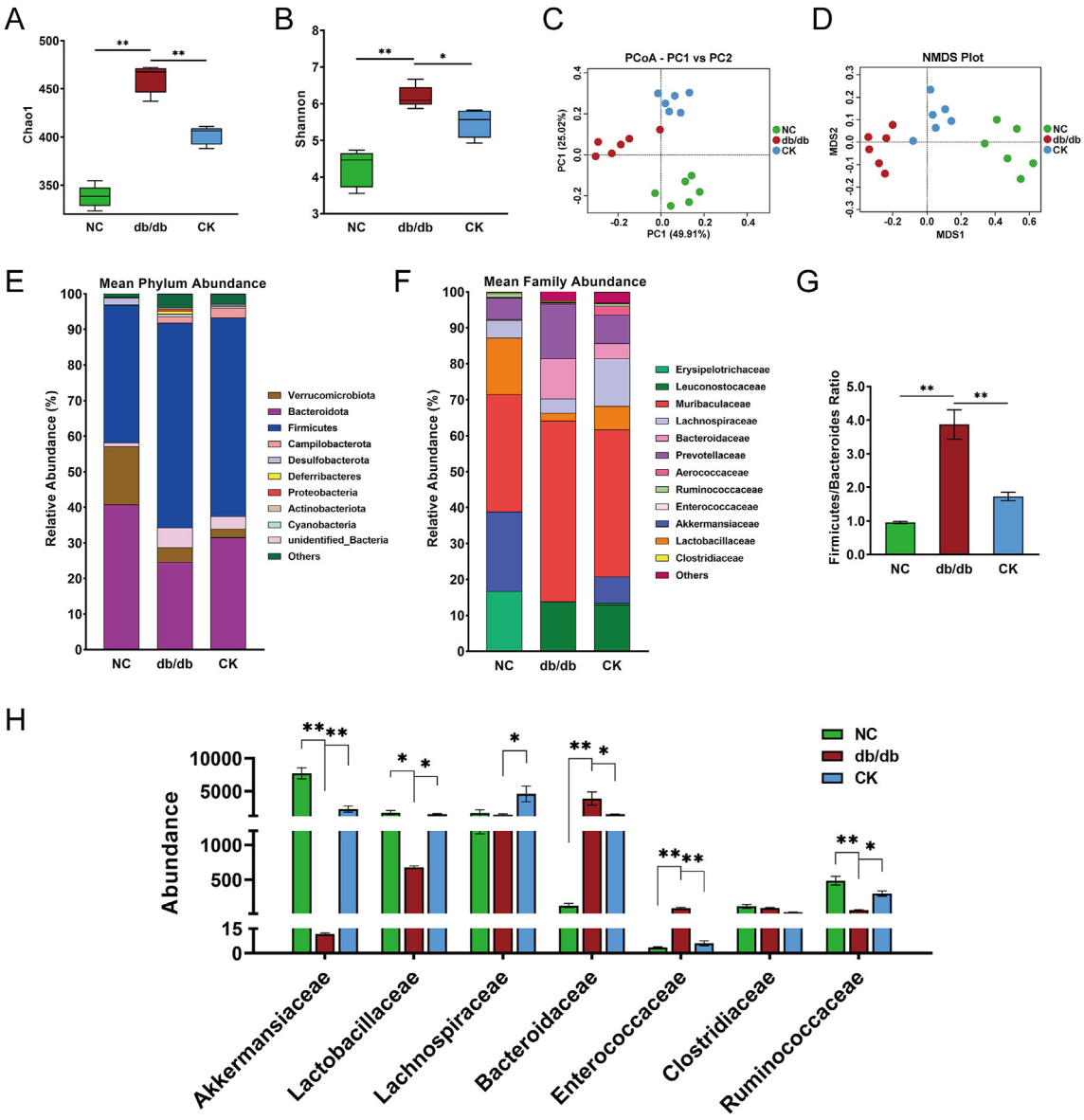

Fig. 2. The alteration of gut microbiota in response to CK treatment. The α diversity analysis were evaluated through Chao1 (A) and Shannon (B) index of metagenomic sequencing data. PCoA (C) and NMDS (D) were plotted among groups. Relative abundance of taxa at the phylum taxonomic level (E) and family taxonomic level (F). Firmicutes/Bacteroidetes ratio (G). Relative abundance of Akkermansiaceae, Lactobacillaceae, Lachnospiraceae, Bacteroidaceae, Enterococcaceae, Clostridiaceae, and Ruminococcaceae (H). Data are presented as the mean ± s.e.m., n = 6 per group. $^{*}P < 0.05$, $^{**}P < 0.01$ versus the db/db group.

expression levels of Hes1 and Math1 were analyzed. Hyperglycemia downregulated the expression of Math1, while CK led to a partial recovery of Math1 expression; however, no changes in Hes1 expression were observed (Fig. 5A), thereby implying that CK targets secretory cells and amplifies their proportion. To further investigate whether CK could increase L-cell numbers, an immunofluorescence assay was performed, and the mature L-cells were labeled with Gcg. L-cell numbers (Gcg-positive cells) were significantly lower in db/db mice compared to the controls, but the cells were partially recovered by CK administration (Fig. 5B and C), corroborating the results from real-time PCR (Fig. 5D). Ngn3, NeuroD1, Foxa1, Foxa2, and Arx are transcription factors governing secretory cell lineage differentiation into L-cells. Earlier studies show that TGR5 signaling drives these transcription factors to facilitate this differentiation into L-cells [15]. Downregulation of these transcription factors was observed in db/db mice. However, these factors were partially restored in response to CK treatment, with the exception of Arx (Fig. 5D). Thus, the data indicate that CK can drive L-cell number expansion in db/db mice.

4. Discussion

Based on previous studies on the BA pool derived by gut microbiota, a general mechanism was proposed, whereby the ginsenoside CK promoted the differentiation of L-cells and expanded the L-cell population of the intestinal epithelium to fundamentally alleviate incretin impairment via amplified GLP-1 secretion. Previous experiments have linked CK consumption to the increased release of GLP-1 in NCI–H716 cells. Encouraged by the results of in vitro experiments, the detailed mechanism underlying this process in the db/db group was investigated. Herein, CK, a bioactive ginsenoside Rb1 metabolite, markedly enhanced the impaired glucose tolerance in the db/db group by relying on the remodeling of the gut microbiota and BA profiles. In particular, CK intervention

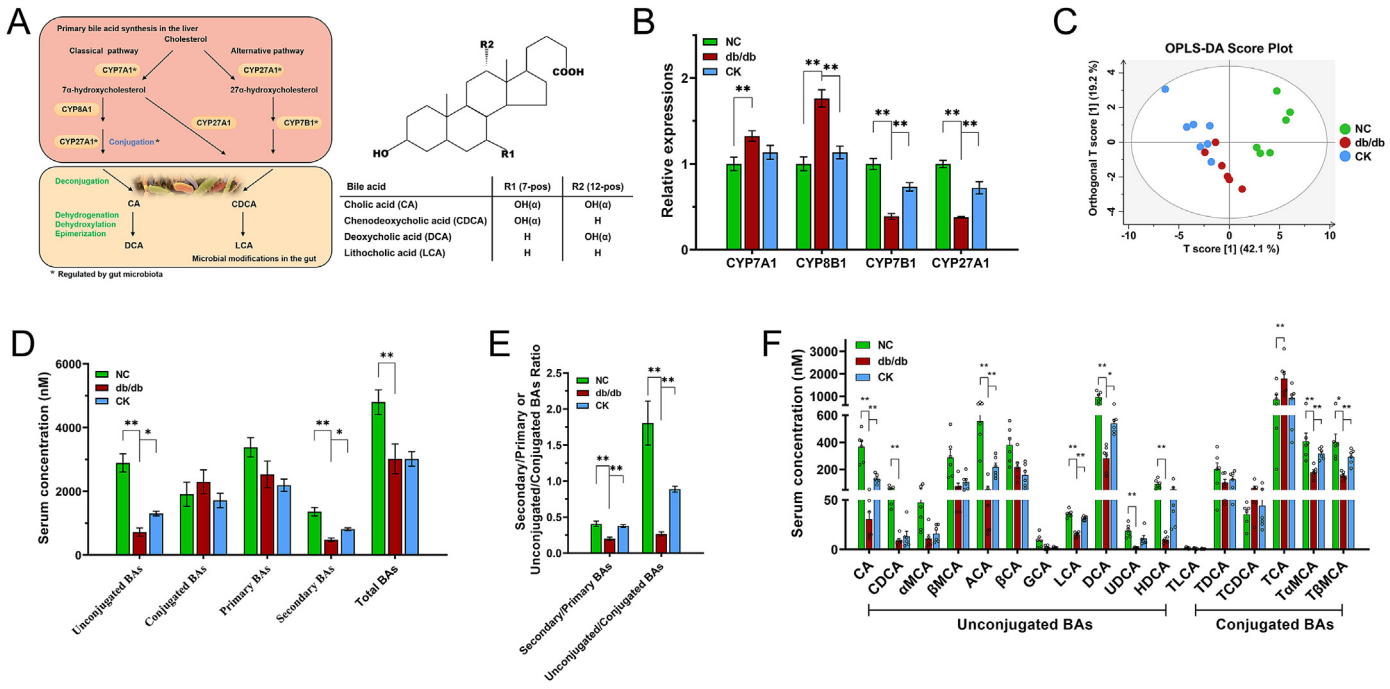

Fig. 3. Altered serum bile acid profiles and bile acid biosynthesis by CK intervention in db/db mice. Schematic diagram of the classical and alternative bile acid biosynthesis pathways (A). RT-qPCR analysis of key enzymes in bile acid synthesis and transporters in the liver (B). OPLS-DA score plots of BA in serum (C). Serum total BA, unconjugated BA,conjugated BA, primary BA, and secondary BA levels (D). The ratios of unconjugated to conjugated, and secondary to primary BA (E). Altered serum BA profiles induced by oral administration of CK for 4 weeks in db/db mice (F). Data are presented as the mean ± s.e.m., n = 6 per group. *$P < 0.05$, **$P < 0.01$ versus the db/db group.

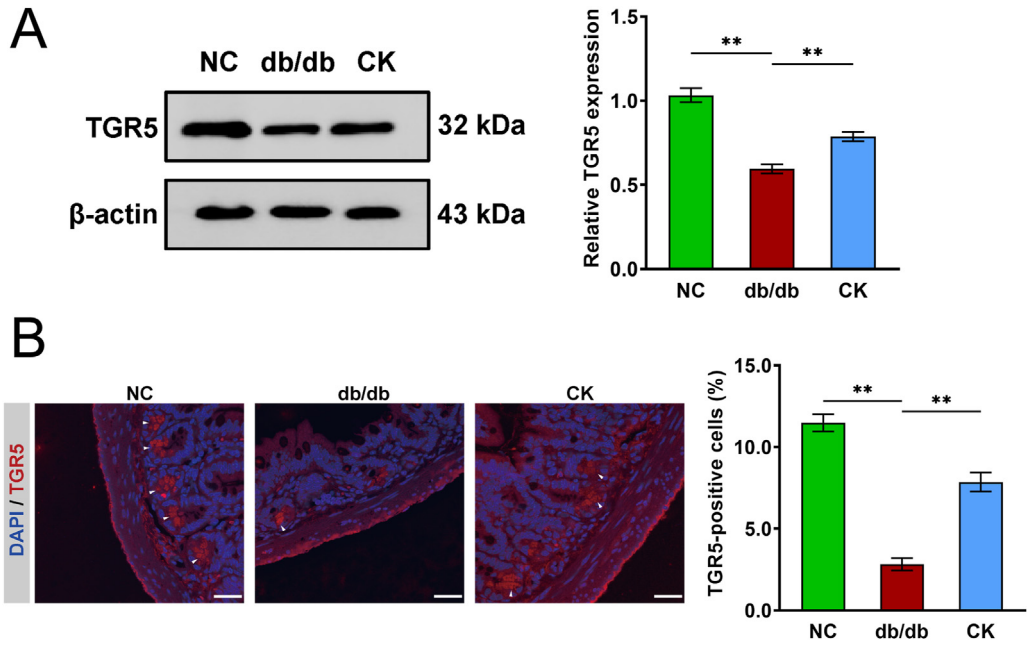

Fig. 4. Metabolic benefits of CK leans on the TGR5 activation. The expression levels of TGR5, and β-actin in ileum samples were evaluated by Western blot analysis, and densitometric analysis was applied to quantify the expression levels of TGR5 (A). Detection of TGR5 for plasma membrane staining in mouse ileum and percentage of TGR5-positive cells (B). Nucleus labeling by DAPI (blue). White arrows indicate positive TGR5 staining outside of the epithelial layer. Scale bars, 25 μm. Data are presented as the mean ± s.e.m., n = 3 per group. *$P < 0.05$, **$P < 0.01$ versus the db/db group.

contributed to the upregulation of the alternative pathway of BA synthesis, stimulating secondary BAs release, especially LCA and DCA. Downstream TGR5 activation, supported by the upregulation of transcription factors guiding L-cell differentiation, is sufficient to coordinate L-cell population expansion. Altogether, these results further substantiate the hypothesis that the reinforcing effect of CK on glucose metabolism and insulin sensitivity could enhance GLP-1 secretion via an increase in L-cell abundance.

CK with high water solubility is more potent than that of the other precursors as it is thus more likely to be absorbed in the

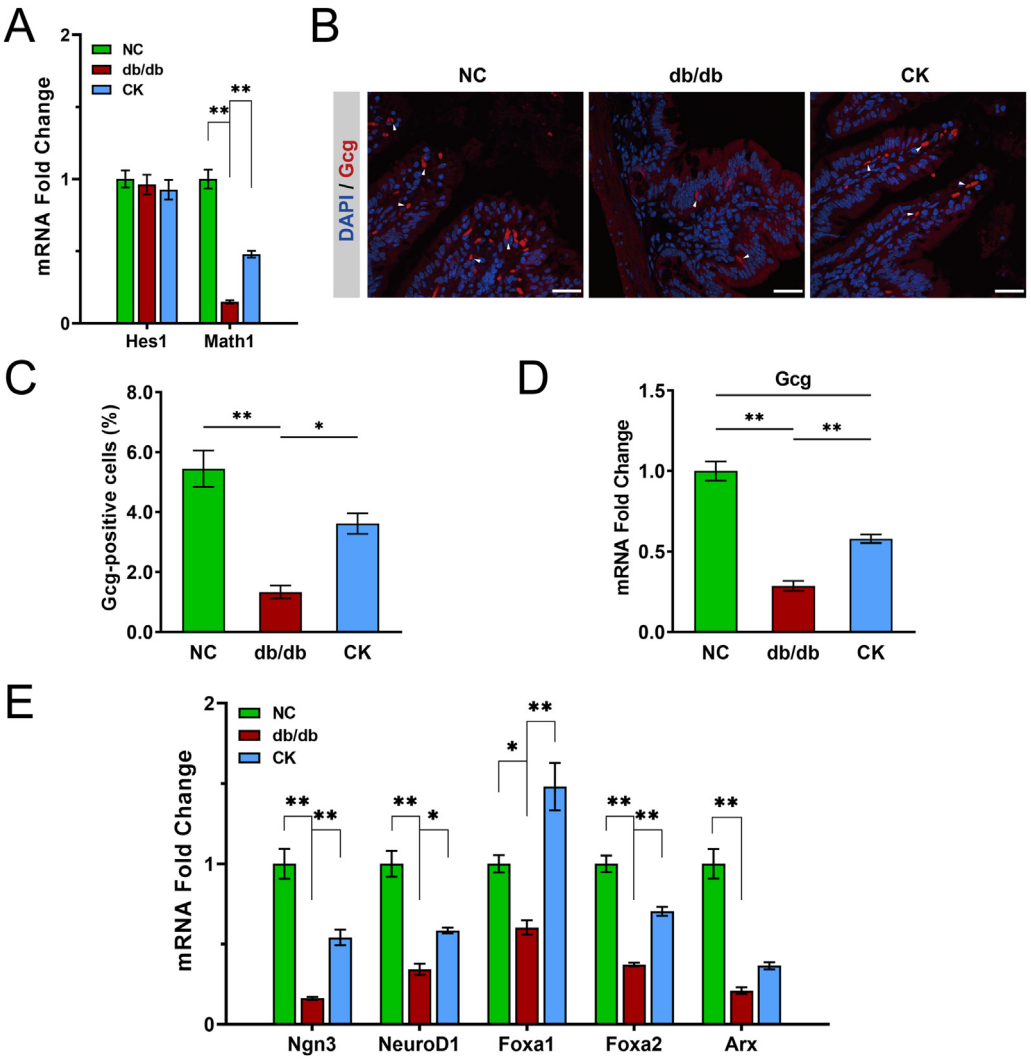

Fig. 5. CK promotes more cells converting into more GLP-1 producing. Gene expression of cell type markers of secretory and absorptive cells (A). Gcg^{+} cells in the ileum of control, db/db, and CK-treated mice (B). Nuclei labeled by DAPI. Scale bars, 25 μm. White arrows indicate positive Gcg staining. Percentage of Gcg-positive cells (C). Gcg expression in mouse ileum (D). Gene expression of intestinal cell type markers and transcription factors directing L-cell development (F). Data are presented as the mean ± s.e.m., n = 3 per group. $^{*}P < 0.05$, $^{**}P < 0.01$ versus the db/db group.

intestine and exert its anti-hyperglycemic and anti-inflammatory effects [17,27]. It has been reported to present an antidiabetic effect similar to metformin in response to insulin resistance and hyperglycemia [28]. Herein, CK decreased the *Firmicutes/Bacteroides* ratio associated with the diabetic phenotype. The enrichment of *Akkermansiaceae and Lachnospiraceae* families contributes to the maintenance of gut barrier functions by attenuating inflammation [29,30], and CK may sustain their abundances via its anti-inflammatory properties to exhibit metabolic benefits. CK may also achieve metabolic benefits via *Lactobacillaceae* enrichment, which can elevate antimicrobial peptide levels in the ileum [31]. In addition, the rise in *Bacteroidaceae* is reported to induce the mucosal inflammation in the intestinal lining [32] and potentially exacerbate incretin impairment. *Ruminococcacea* can convert primary BAs to LCA and DCA via a multi-step 7α-dehydroxylation reaction [24]. In this study, the decrease in *Ruminococcacea* in db/db mice was reversed by CK remodels the gut microbiota and further impacts BA pool size and profile.

Metabolic defects in the microbiota-BA axis may serve as an essential link in the incretin impairment, further impinging upon the intestinal milieu. During the promotion of fecal BA output, the conversion of primary BAs to secondary BAs drives the stimulation of GLP-1 [33]. Considering that alterations in BA biosynthetic pathways are tightly related to the host metabolism, the alternative pathway is upregulated through depleting CYP8B1, thereby enhancing glucose tolerance by increasing GLP-1 secretion in a BA-dependent manner [34]. Furthermore, a striking predominance of the alternative pathway in BA synthesis was noted after CK treatment and confirmed by the upregulation of CYP7B1 and CYP27A1, which might contribute to the subsequent increase in secondary BAs, particularly LCA. This is supported by the rise in secondary BAs that appears to stimulate GLP-1 secretion through basolateral intestinal TGR5 activation in the L-cells, independent of BA conjugation status [25]. Mechanistically, the alternative pathway plays a key signaling role in secondary BA synthesis during CK intervention.

Previous studies have described that the role of TGR5 in alleviating obesity-related dysregulation of glucose tolerance and insulin resistance is by triggering conversion of white fat to brown fat, thereby leading to increased energy expenditure via thermogenesis [35]. In this study, weight loss and improved glycolipid metabolism resulting from CK administration might be attributed to this

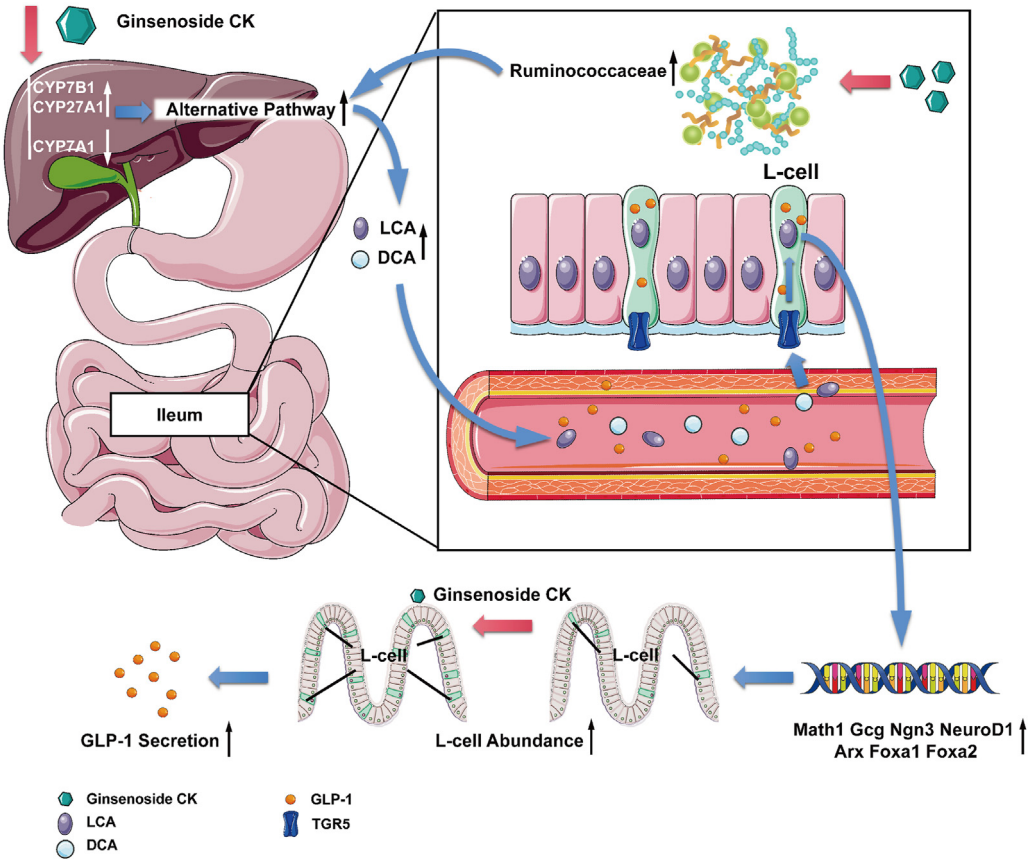

Fig. 6. Diagram illustrating a proposed mechanism by which CK stimulates GLP-1 secretion through gut microbiota-BA-TGR5 axis.

mechanism. As chronic low-grade inflammation introduced through hyperglycemia undermines mucosal morphology with reduced integrity of adherence and tight junctions and exacerbates metabolic dysfunction [36,37], TGR5 likely contributes to the metabolic benefits involved in the repair of the intestinal epithelial damage by virtue of its anti-inflammatory action. LCA protects the epithelial barrier by inhibiting the release of various pro-inflammatory factors [38], and its supplementation replenishes physiological levels of BAs that leads to the overall alleviation of colitis-induced damage of the intestinal epithelium through a mechanism involving TGR5-dependent anti-inflammatory actions [39]. Moreover, TGR5 has recently been shown to coordinate of cell renewal and specification among the subpopulation of the intestinal epithelium [40], particularly L-cells [15]. These findings, together with the results of this study, signal that CK compensates for the impaired incretin effect by expanding L-cell abundance through the BA-TGR5 molecular axis.

Modulation of L-cell differentiation represents a therapeutically applicable target that enforces conversion of more intestinal epithelial cells into GLP-1-producing cells. The overexpression of Math1 with CK treatment also supports this mechanism of action, with no differences in absorptive lineage proportion, potentially attributed to the complexity in detecting transient changes in the Hes1 level [3]. Interestingly, L-cell population grew by an appreciable amount in vitro and in vivo by blocking the Notch signaling, accompanied by a net increase in secretory cells [41]. This positive effect is also produced by TGR5 activation. A recent study on the relationship between the two uncovered that TGR5 activation, mediated by LCA and DCA, ultimately suppresses Notch expression, leading to a significant amelioration in metabolic disturbances [42]. Together with the data from L-cell differentiation, this suggests that CK facilitates the amplification of L-cell numbers, and this conversion trend is established in the initial lineage commitment phase and not merely forcing the start of Gcg synthesis in late endocrine precursors. These findings provide novel insights into the potential mechanisms underlying the beneficial effects of CK on enteroendocrine expansion and indicate that secondary BAs could be required to initiate the TGR5-dependent regenerative process.

5. Conclusion

In conclusion, this study demonstrated that CK might act as a TGR5 agonist to alleviate hyperglycemia and insulin resistance, with the accumulation of LCA and DCA resulting from an increase in the abundance of *Ruminococcaceae* in db/db mice. CK not only stimulated GLP-1 secretion but also increased L-cell numbers and promoted general differentiation into EEC lineage, thereby conferring metabolic benefits in obesity-diabetes (Fig. 6). Hence, CK represents an innovative compound, and the remodeling of the gut microbiota in favor of microorganisms producing BAs to activate TGR5 locally serves as a promising therapeutic target for abnormal glucose homeostasis.

Declaration of competing interest

The authors declare that they have no conflicts of interest.

Acknowledgements

This work was supported by the National Key Research and Development Program of China (2018YFC2000200), The National Natural Science Foundation of China (82174131), Zhejiang Provincial Natural Science Foundation of China (LY21H030002), and the Medical Health Science and Technology Project of Zhejiang Provincial Health Commission (2019RC229).

Appendix A. Supplementary data

Supplementary data to this article can be found online at https://doi.org/10.1016/j.jgr.2022.03.006.

References

[1] Drucker DJ, Nauck MA. The incretin system: glucagon-like peptide-1 receptor agonists and dipeptidyl peptidase-4 inhibitors in type 2 diabetes. Lancet 2006;368:1696–705.
[2] Basak O, Beumer J, Wiebrands K, Seno H, van Oudenaarden A, Clevers H. Induced quiescence of Lgr5+ stem cells in intestinal organoids enables differentiation of hormone-producing enteroendocrine cells. Cell Stem Cell 2017;20:177–190 e4.
[3] Petersen N, Frimurer TM, Terndrup Pedersen M, Egerod KL, Wewer Albrechtsen NJ, Holst JJ, Grapin-Botton A, Jensen KB, Schwartz TW. Inhibiting RHOA signaling in mice increases glucose tolerance and numbers of enteroendocrine and other secretory cells in the intestine. Gastroenterology 2018;155:1164–11676 e2.
[4] Gehart H, Clevers H. Tales from the crypt: new insights into intestinal stem cells. Nat Rev Gastroenterol Hepatol 2019;16:19–34.
[5] Clevers H. The intestinal crypt, a prototype stem cell compartment. Cell 2013;154:274–84.
[6] Gradwohl G, Dierich A, LeMeur M, Guillemot F. neurogenin3 is required for the development of the four endocrine cell lineages of the pancreas. Proc Natl Acad Sci U S A 2000;97:1607–11.
[7] Naya FJ, Huang HP, Qiu Y, Mutoh H, DeMayo FJ, Leiter AB, Tsai MJ. Diabetes, defective pancreatic morphogenesis, and abnormal enteroendocrine differentiation in BETA2/neuroD-deficient mice. Genes Dev 1997;11:2323–34.
[8] Ye DZ, Kaestner KH. Foxa1 and Foxa2 control the differentiation of goblet and enteroendocrine L- and D-cells in mice. Gastroenterology 2009;137:2052–62.
[9] Morimoto K, Watanabe M, Sugizaki T, Irie J, Itoh H. Intestinal bile acid composition modulates prohormone convertase 1/3 (PC1/3) expression and consequent GLP-1 production in male mice. Endocrinology 2016;157:1071–81.
[10] Sato T, Clevers H. Growing self-organizing mini-guts from a single intestinal stem cell: mechanism and applications. Science 2013;340:1190–4.
[11] Komaroff AL. The microbiome and risk for obesity and diabetes. JAMA 2017;317:355–6.
[12] Wahlstrom A, Sayin SI, Marschall HU, Backhed F. Intestinal crosstalk between bile acids and microbiota and its impact on host metabolism. Cell Metabol 2016;24:41–50.
[13] Jadhav K, Xu Y, Xu Y, Li Y, Xu J, Zhu Y, Adorini L, Lee YK, Kasumov T, Yin L, et al. Reversal of metabolic disorders by pharmacological activation of bile acid receptors TGR5 and FXR. Mol Metabol 2018;9:131–40.
[14] Deutschmann K, Reich M, Klindt C, Droge C, Spomer L, Haussinger D, Keitel V. Bile acid receptors in the biliary tree: TGR5 in physiology and disease. Biochim Biophys Acta (BBA) - Mol Basis Dis 2018;1864:1319–25.
[15] Lund ML, Sorrentino G, Egerod KL, Kroone C, Mortensen B, Knop FK, Reimann F, Gribble FM, Drucker DJ, de Koning EJP, et al. L-cell differentiation is induced by bile acids through GPBAR1 and paracrine GLP-1 and serotonin signaling. Diabetes 2020;69:614–23.
[16] Kim DH. Gut microbiota-mediated pharmacokinetics of ginseng saponins. J Ginseng Res 2018;42:255–63.
[17] Chen W, Wang J, Luo Y, Wang T, Li X, Li A, Li J, Liu K, Liu B. Ginsenoside Rb1 and compound K improve insulin signaling and inhibit ER stress-associated NLRP3 inflammasome activation in adipose tissue. J Ginseng Res 2016;40:351–8.
[18] Kim K, Park M, Lee YM, Rhyu MR, Kim HY. Ginsenoside metabolite compound K stimulates glucagon-like peptide-1 secretion in NCI-H716 cells via bile acid receptor activation. Arch Pharm Res (Seoul) 2014;37:1193–200.
[19] Tian F, Wang X, Ni H, Feng X, Yuan X, Huang Q. The ginsenoside metabolite compound K stimulates glucagon-like peptide-1 secretion in NCI-H716 cells by regulating the RhoA/ROCKs/YAP signaling pathway and cytoskeleton formation. J Pharmacol Sci 2021;145:88–96.
[20] Song W, Wei L, Du Y, Wang Y, Jiang S. Protective effect of ginsenoside metabolite compound K against diabetic nephropathy by inhibiting NLRP3 inflammasome activation and NF-kappaB/p38 signaling pathway in high-fat diet/streptozotocin-induced diabetic mice. Int Immunopharm 2018;63:227–38.
[21] Yang L, Xiong A, He Y, Wang Z, Wang C, Wang Z, Li W, Yang L, Hu Z. Bile acids metabonomic study on the CCl4- and alpha-naphthylisothiocyanate-induced animal models: quantitative analysis of 22 bile acids by ultraperformance liquid chromatography-mass spectrometry. Chem Res Toxicol 2008;21:2280–8.
[22] Sun L, Pang Y, Wang X, Wu Q, Liu H, Liu B, Liu G, Ye M, Kong W, Jiang C. Ablation of gut microbiota alleviates obesity-induced hepatic steatosis and glucose intolerance by modulating bile acid metabolism in hamsters. Acta Pharm Sin B 2019;9:702–10.
[23] Sayin SI, Wahlstrom A, Felin J, Jantti S, Marschall HU, Bamberg K, Angelin B, Hyotylainen T, Oresic M, Backhed F. Gut microbiota regulates bile acid metabolism by reducing the levels of tauro-beta-muricholic acid, a naturally occurring FXR antagonist. Cell Metabol 2013;17:225–35.
[24] Vital M, Rud T, Rath S, Pieper DH, Schluter D. Diversity of bacteria exhibiting bile acid-inducible 7alpha-dehydroxylation genes in the human gut. Comput Struct Biotechnol J 2019;17:1016–9.
[25] Kuhre RE, Wewer Albrechtsen NJ, Larsen O, Jepsen SL, Balk-Moller E, Andersen DB, Deacon CF, Schoonjans K, Reimann F, Gribble FM, et al. Bile acids are important direct and indirect regulators of the secretion of appetite- and metabolism-regulating hormones from the gut and pancreas. Mol Metabol 2018;11:84–95.
[26] Dong S, Zhu M, Wang K, Zhao X, Hu L, Jing W, Lu H, Wang S. Dihydromyricetin improves DSS-induced colitis in mice via modulation of fecal-bacteria-related bile acid metabolism. Pharmacol Res 2021;171:105767.
[27] Lu S, Luo Y, Zhou P, Yang K, Sun G, Sun X. Ginsenoside compound K protects human umbilical vein endothelial cells against oxidized low-density lipoprotein-induced injury via inhibition of nuclear factor-kappaB, p38, and JNK MAPK pathways. J Ginseng Res 2019;43:95–104.
[28] Hwang YC, Oh DH, Choi MC, Lee SY, Ahn KJ, Chung HY, Lim SJ, Chung SH, Jeong IK. Compound K attenuates glucose intolerance and hepatic steatosis through AMPK-dependent pathways in type 2 diabetic OLETF rats. Korean J Intern Med 2018;33:347–55.
[29] Cao H, Li C, Lei L, Wang X, Liu S, Liu Q, Huan Y, Sun S, Shen Z. Stachyose improves the effects of berberine on glucose metabolism by regulating intestinal microbiota and short-chain fatty acids in spontaneous type 2 diabetic KKAy mice. Front Pharmacol 2020;11:578943.
[30] Harrison CA, Laubitz D, Ohland CL, Midura-Kiela MT, Patil K, Besselsen DG, Jamwal DR, Jobin C, Ghishan FK, Kiela PR. Microbial dysbiosis associated with impaired intestinal Na(+)/H(+) exchange accelerates and exacerbates colitis in ex-germ free mice. Mucosal Immunol 2018;11:1329–41.
[31] Ojo BA, O'Hara C, Wu L, El-Rassi GD, Ritchey JW, Chowanadisai W, Lin D, Smith BJ, Lucas EA. Wheat germ supplementation increases Lactobacillaceae and promotes an anti-inflammatory gut milieu in C57bl/6 mice fed a high-fat, high-sucrose diet. J Nutr 2019;149:1107–15.
[32] Bloom SM, Bijanki VN, Nava GM, Sun L, Malvin NP, Donermeyer DL, Dunne Jr WM, Allen PM, Stappenbeck TS. Commensal Bacteroides species induce colitis in host-genotype-specific fashion in a mouse model of inflammatory bowel disease. Cell Host Microbe 2011;9:390–403.
[33] Fuchs CD, Paumgartner G, Mlitz V, Kunczer V, Halilbasic E, Leditznig N, Wahlstrom A, Stahlman M, Thuringer A, Kashofer K, et al. Colesevelam attenuates cholestatic liver and bile duct injury in Mdr2(-/-) mice by modulating composition, signalling and excretion of faecal bile acids. Gut 2018;67:1683–91.
[34] Kaur A, Patankar JV, de Haan W, Ruddle P, Wijesekara N, Groen AK, Verchere CB, Singaraja RR, Hayden MR. Loss of Cyp8b1 improves glucose homeostasis by increasing GLP-1. Diabetes 2015;64:1168–79.
[35] Wu Q, Liang X, Wang K, Lin J, Wang X, Wang P, Zhang Y, Nie Q, Liu H, Zhang Z, et al. Intestinal hypoxia-inducible factor 2alpha regulates lactate levels to shape the gut microbiome and alter thermogenesis. Cell Metabol 2021;10:1988–2003.
[36] Burcelin R. Gut microbiota and immune crosstalk in metabolic disease. Mol Metabol 2016;5:771–81.
[37] Daryabor G, Atashzar MR, Kabelitz D, Meri S, Kalantar K. The effects of type 2 diabetes mellitus on organ metabolism and the immune system. Front Immunol 2020;11:1582.

[38] Ward JBJ, Lajczak NK, Kelly OB, O'Dwyer AM, Giddam AK, Ni Gabhann J, Franco P, Tambuwala MM, Jefferies CA, Keely S, et al. Ursodeoxycholic acid and lithocholic acid exert anti-inflammatory actions in the colon. Am J Physiol Gastrointest Liver Physiol 2017;312:G550–8.

[39] Sinha SR, Haileselassie Y, Nguyen LP, Tropini C, Wang M, Becker LS, Sim D, Jarr K, Spear ET, Singh G, et al. Dysbiosis-induced secondary bile acid deficiency promotes intestinal inflammation. Cell Host Microbe 2020;27:659–670 e5.

[40] Sorrentino G, Perino A, Yildiz E, El Alam G, Bou Sleiman M, Gioiello A, Pellicciari R, Schoonjans K. Bile acids signal via TGR5 to activate intestinal stem cells and epithelial regeneration. Gastroenterology 2020;159:956–968 e8.

[41] Petersen N, Reimann F, van Es JH, van den Berg BM, Kroone C, Pais R, Jansen E, Clevers H, Gribble FM, de Koning EJ. Targeting development of incretin-producing cells increases insulin secretion. J Clin Invest 2015;125:379–85.

[42] Chen YS, Liu HM, Lee TY. Ursodeoxycholic acid regulates hepatic energy homeostasis and white adipose tissue macrophages polarization in leptin-deficiency obese mice. Cells 2019;8.